Final

FINAL REPORT

ERIP INVENTION #668
CONTRACT DE-FG01-97EE15668 INITIATED 7/21/97
FLOW INTEGRATING SECTION FOR A GAS TURBINE ENGINE IN WHICH TURBINE BLADES ARE COOLED BY FULL COMPRESSOR FLOW

Submitted to: DOE Project Officer, David Crouch
1000 independence Ave. SW
Washington, DC 20585 - 2 copies

Office of Placement & Administration, HR-542
Sara Wilson
1000 Independence Ave. SW
Washington, DC 20585 - 1 copy

U.S. Department of Energy
Office of Scientific and Technical Information
P.O. Box 62
Oak Ridge, TN 37830 - 1 copy

By: Dr. W. Gene Steward
FluidTherm Engineering
169 S. Peak Lane
Boulder, CO 80302

(303) 444 0875
(303) 444 6548 FAX
steward@denver.net

Submitted: 11/14/99

DISCLAIMER

CONTENTS

SECTION	PAGE
1. BACKGROUND SUMMARY	1
1.1 THE EXISTING TECHNOLOGY	
1.2 THE FULL FLOW COOLING PRINCIPLE	2
1.3 FEASIBILITY AND BENEFITS OF FULL FLOW TURBINE BLADE COOLING AND REGENERATION - SBIR PHASE I	3
1.4 COMPARISON OF ENGINE TYPES	6
1.5 THE FLOW INTEGRATING SECTION - ERIP INVENTION	7
2. THE ERIP PROJECT	9
2.1 ERIP PROJECT - CFD (Computational Fluid Dynamics Modeling)	9
2.2 ERIP PROJECT - EXPERIMENTAL PHASE	13
2.3 COMPARISONS OF COMPUTED AND EXPERIMENTAL RESULTS	17
3. COMMERCIAL POSSIBILITIES AND SPECIAL CONSIDERATIONS FOR VERY SMALL ENGINES	17
4. EFFECTS OF SMALL SIZE ON FIS DESIGN	18
5. CONCLUSIONS CONCERNING THE FLOW INTEGRATING SECTION	21
5. COMMERCIALIZATION	23
6. REFERENCES	24

1. BACKGROUND SUMMARY:

SBIR Phase I Study: An innovation in gas turbine engine design, which was the subject of a 1991 SBIR Phase 1 study [1] by FTE, would increase efficiency by maximizing the cooling of turbine blades, thus allowing them to operate at far greater turbine inlet gas temperature than is possible with current cooling methods. Consolidation of the two major components, turbine and compressor, to route all of the compressor airflow through hollow turbine blades would also result in an unusually compact engine configuration. The SBIR study, and subsequent work, indicate that efficiency gain due to increased turbine inlet temperature, greatly outweighs the adverse effects of heat transfer during compression and expansion. With the use of state-of-the art high temperature materials and regeneration (utilization of waste exhaust heat) the engine could compete with or surpass the most efficient of piston engines on the basis of performance and fuel consumption alone.

ERIP Invention: This applicant's attempt to patent the full flow turbine blade cooling concept encountered two forty year old prior patents[2,3]; however, neither of these inventions addressed a serious problem which seemed certain to disable the compressor diffuser and make the engine unworkable. The present Energy Related Invention Program (ERIP) grant was awarded to FTE in 1997 to develop and test an invention, a "Flow Integrating Section" (FIS), which is intended to alleviate the diffuser flow problem. The ERIP project started with a preliminary FIS design based on a classic boundary layer solution for free jet flow. Computational fluid dynamic modeling[4] of many variations of FIS geometry led to an optimization of the design which was then tested by a series of experiments at Colorado Engineering Experiment Station (CEESI)[5]. Experiments agreed with the computations to within five points of diffusion efficiency, and near the optimum geometry the agreement was better than one point. The best experimental diffuser efficiency was 84%; computed efficiency being 84.7%. These efficiencies would be very good even for conventional diffusers. The ERIP program established design criteria, and confirmed that the Flow Integrating Section is essential to the operation of the novel engine: when the FIS was removed the diffusion efficiency dropped to 29% experimental, and 25% computed.

1.1 THE EXISTING TECHNOLOGY

The gas turbine engine has great appeal because of its simplicity of principle, high power density, smoothness of operation due to absence of reciprocating components, and ability to operate with a wide variety of fuels. The Brayton (gas turbine) cycle with regeneration (recovery of waste exhaust heat) has Carnot efficiency as its upper limit, the highest efficiency attainable in a heat engine operating between given temperatures of source and sink. While the gas turbine does not reach the peak pressure and temperatures of the Otto cycle or the Diesel cycle engines, it can exploit nearly complete expansion of the gas down to atmospheric pressure, as opposed to piston engines which can only expand the gas through a finite stroke. Most importantly, the gas turbine is unique among open cycle engines in its ability to reclaim a very large fraction of the exhaust gas heat through regeneration. Unfortunately, the gas turbine is one of the furthest from achieving its potential efficiency, and low efficiency has been the main deterrent to nonmilitary use of gas turbine engines under five hundred horsepower.

* superscripted numbers in parentheses indicate references in Section 7

Efficiency and power depend directly on the peak pressure and temperature in the cycle. Consequently, turbine designers have focused on several methods for increasing the allowable peak gas temperature: (1) development of superalloys and ceramic materials which resist corrosion and retain their strength at high temperatures, (2) convective and film cooling of turbine blades by air bled from the compressor, (3) water injection cooling. High temperature materials research has tremendously improved gas turbines; however, the best new materials, in conjunction with current methods of cooling, have not allowed the gas turbine to match the efficiency of other internal combustion engines.

1.2 THE FULL FLOW COOLING PRINCIPLE

Figure 1 shows the essence of the inventions of Helou[2], and Schulz[3]. Hollow, axial flow turbine blades form the periphery of a centrifugal compressor impeller so that the entire flow of compressor air passes through, and cools the hollow turbine blades. Shrouds at the inner and outer blade radii separate the turbine flow passages from the compressor passages. The French patent of Helou employs a single integrated compressor/turbine stage for the jet reaction rather than shaft power – it is a jet engine. The Schulz omits the outer shroud, which eliminates the problem of cooling that portion of the turbine blade passage, but would undesirably mix combustion gas with the discharge flow from the centrifugal compressor. Schulz also introduces a split compressor stage which decreases flow restriction and provides a second turbine stage which relieves the tendency for high turbine loading in this engine. In a centrifugal compressor with straight vanes around half of the pressure rise occurs in the rotor and half in the diffuser. The diffuser as shown in Figure 1 would lose most of its intended pressure rise due to turbulent eddies. The ERIP invention Flow Integrating Section is intended to alleviate this loss.

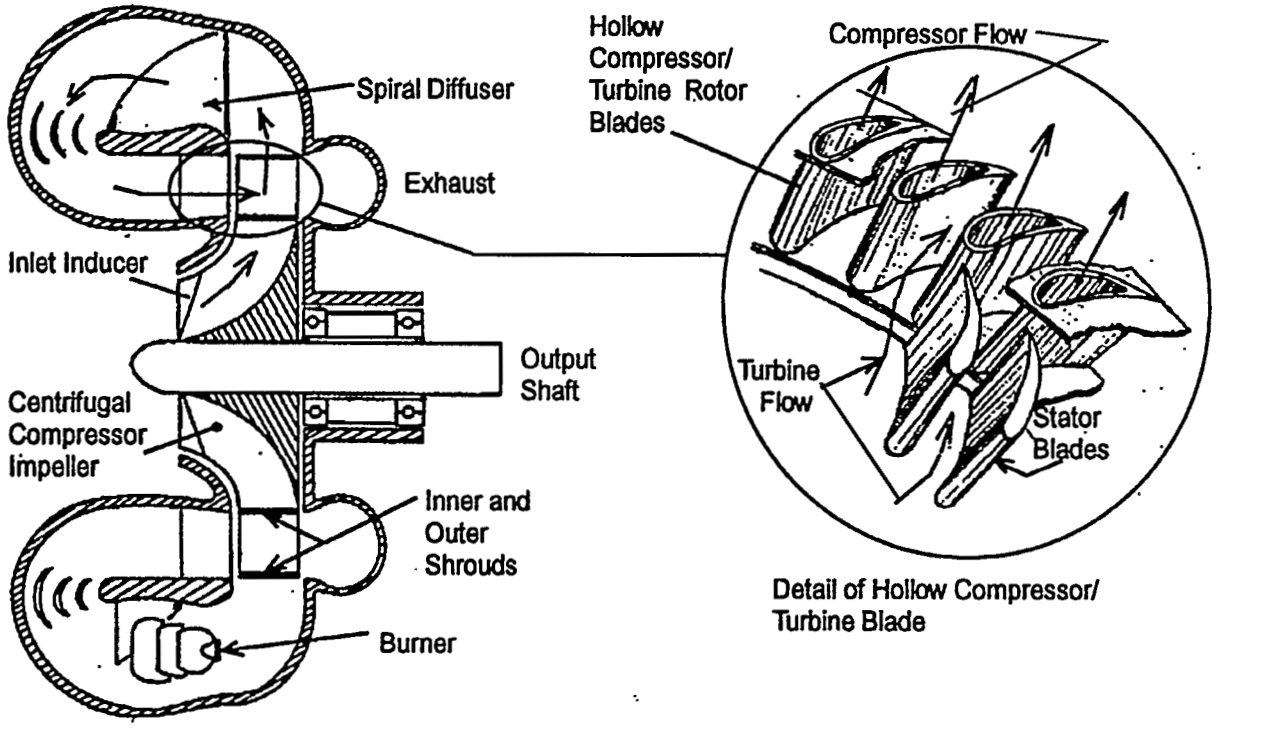

Figure 1. Full flow cooled gas turbine engine (original invention)[2,3]

* superscripted numbers in parentheses indicate references in Section 7

1.3 FEASIBILITY AND BENEFITS OF FULL FLOW TURBINE BLADE COOLING AND REGENERATION - SBIR PHASE I[1]

Note: The diffuser pressure loss problem which led to the "Flow Integrating Section" invention is treated separately in 1.5.

1.3.1 Blade Heat Transfer Effects

There are negative as well as positive effects of extreme cooling of turbine blades. The positive effect is that the higher allowable turbine inlet gas temperature by itself would greatly increase the engine efficiency. The counter effect is that heat transferred into the airstream during compression increases the compression work to achieve a given pressure rise, and heat transfer out of the airstream during expansion in the turbine decreases the available turbine work. The ratio, R, of power without heat transfer to power with heat transfer is derived in [1] (either turbine or compressor):

$$R := \frac{Pr^{\frac{k-1}{k}} - 1}{Pr^{\frac{\gamma-1}{\gamma}} - 1} \cdot \frac{\frac{\gamma-1}{\gamma}}{\left(\frac{k-1}{k}\right)}$$

k = ratio of specific heat at constant pressure to specific heat at constant volume.

γ = the polytropic exponent for the diabatic process

Pr = the pressure ratio

The polytropic exponent is related to the blade heat transfer by the following expression:

$$\frac{\gamma-1}{\gamma} := \frac{\ln\left(Pr^{\frac{k-1}{k}} + \frac{Q}{m \cdot c_p \cdot T_1}\right)}{\ln(Pr)}$$

Q = heat flux, watts

m = mass flowrate, kg/s

c_p = specific heat at constant pressure, j/kg.K

T_1 = compression or expansion starting temp., K

To obtain the heat flux, Q, a special blade external convective heat transfer coefficient by Ainley[6] was used, and an internal coefficient by Dittus-Boelter[7]. Through these correlations, Q is a function of the blade surface area, gas Prandtl Number, and Reynolds Number. Figure 2 is an example of power ratio calculations for the engine geometry in reference [1].

* superscripted numbers in parentheses indicate references in Section 7

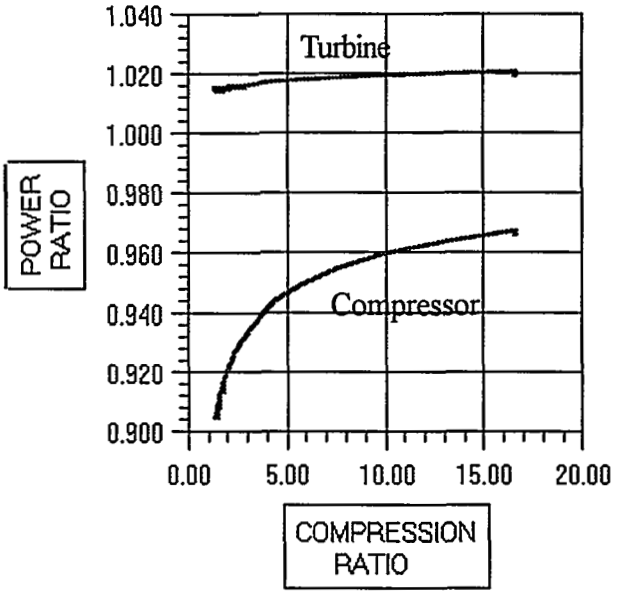

Figure 2. Ratio of power without and with heat transfer. Turbine Inlet Temperature = 1800K.

Figure 3 shows the advantage of full flow cooling with respect to no cooling and partial bleed cooling. All calculations assume a maximum blade temperature of 1100K, for which previous calculations determined that full flow cooling would permit a turbine inlet gas temperature, T_3, of approximately 1800K; 4% compressor bleed cooling, 1225K; and no cooling, 1100K.

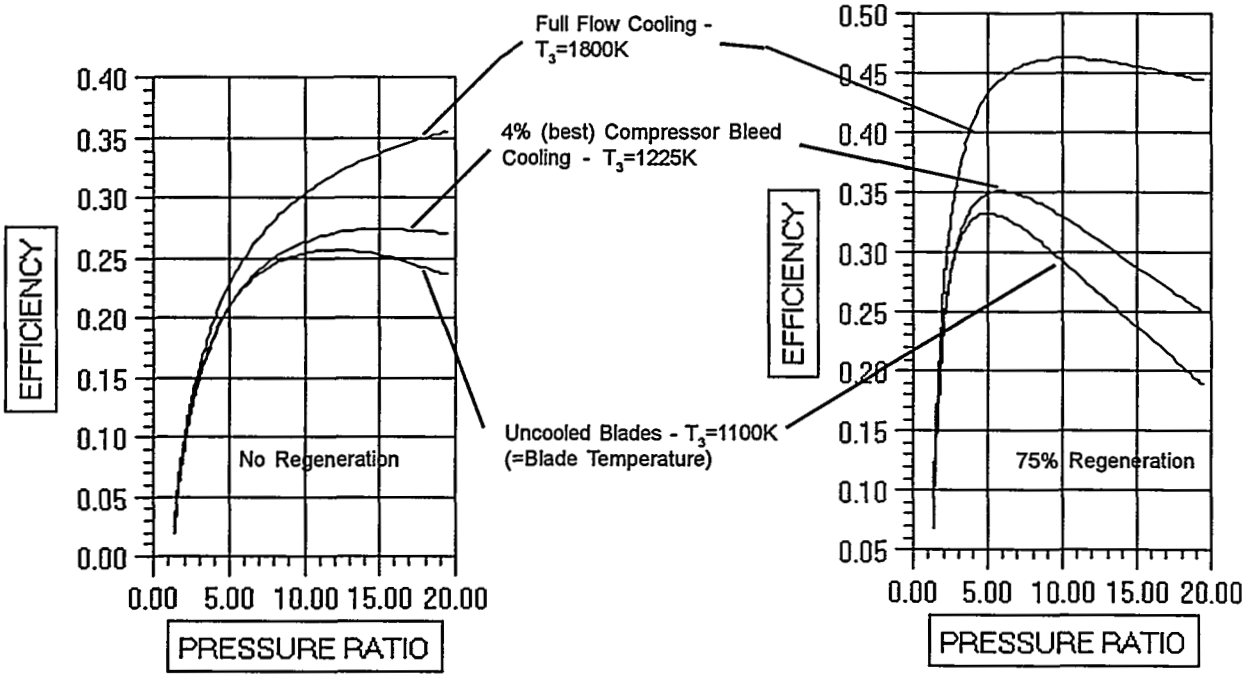

Figure 3. The advantage of full flow turbine blade cooling for a simple Brayton Cycle (no regeneration), and for an engine with 75% effective regeneration. Blade temperature = 1100K in all cases.

* superscripted numbers in parentheses indicate references in Section 7

1.3.2 Benefits of Regeneration with Full Flow Cooling.

Figure 3 allows a comparison between engine efficiency with 75% regeneration, and with no regeneration. Figure 4 shows the effect of degree of regeneration (exhaust heat actually transferred / maximum possible heat transfer) combined with full flow cooling. The following table from reference (8) indicates that regenerator effectiveness (or efficiency) of 90% as claimed by Chrysler is possible (but may be questionable), and all the examples exceeded 75%. The curves of Figure 4 help explain why particular engine configurations are chosen for various applications. Since regenerators and recuperators add bulk, applications which require the ultimate power-to-weight ratio tend toward very high pressure ratio and little or no regeneration. Power density is also higher at higher pressure ratios.

Regeneration is linked to lower pressure ratios because at high pressure ratio the compressor discharge is already hot from compression, and the exhaust gas is cooler because of the greater expansion ratio, so the temperature difference to drive heat transfer diminishes with increasing pressure ratio. In small engines the choice also tends toward lower pressure ratio and regeneration because small engines suffer more from the detrimental effects of high pressure leakage and recirculation. High pressure ratio means high RPM, high centrifugal stress, many stages, close tolerances, and complexity, all of which add to the cost and detract from reliability.

In Table 1 it should be explained that the term "regenerator" is rather ambiguous. "Regenerator" is a general term for all exhaust heat recovery devices, but when speaking of specific types, a regenerator is usually a revolving drum or disk containing an open matrix or honeycomb structure of material having high heat capacity. The structure revolves so that exhaust and compressor discharge air alternately pass through the same material. Heat is absorbed and stored in the material during the exhaust flow, then heat is released to the cooler air flowing through in the opposite direction. A heat exchanger in which heat is conducted through a separating wall, usually with area extending fins, is called a "recuperator".

Table 1. (Table 5.4 in reference [8]) Specifications of several gas turbine engines that have regenerators.

Manufacturer	General Motors	Chrysler	Ford	Rover
Model no.	GT 305	A 831	705	2S/140
Power, bhp	225	130	600	150
Compressor				
Type	Radial	Radial	Radial	Radial
Pressure ratio	3.5	4.1	4.0	3.92
Efficiency (%)	78	80	80	79
Turbine				
Type	Axial	Axial	Axial	Radial
Inlet temp.	1597	1707	1748	1538
Efficiency (%)	84	87	88	86
Regenerator				
Type	Drum matrix	Twin rotating disks	Recup.	Recup.
Effectiveness (%)	86	90	80	78

* superscripted numbers in parentheses indicate references in Section 7

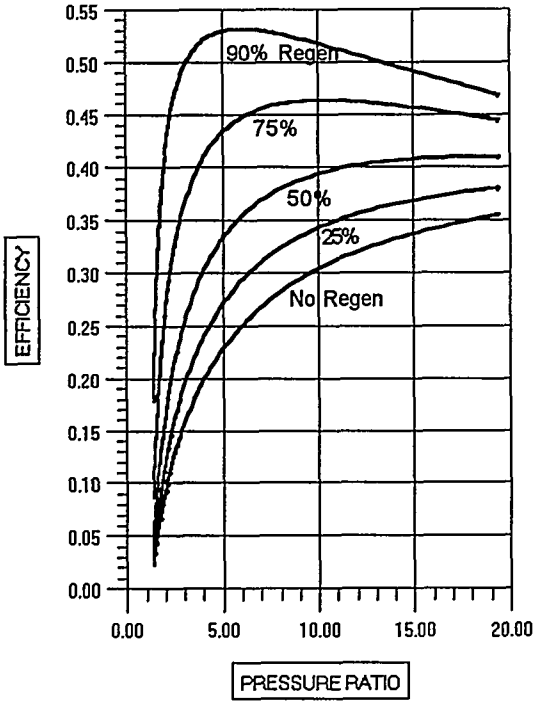

Figure 4. Benefits of regeneration. Turbine inlet temperature = 1800k, with full flow cooling (blade temperature = 1100K).

1.4 COMPARISON OF ENGINE TYPES

REFERENCES

9
10
9
10
1

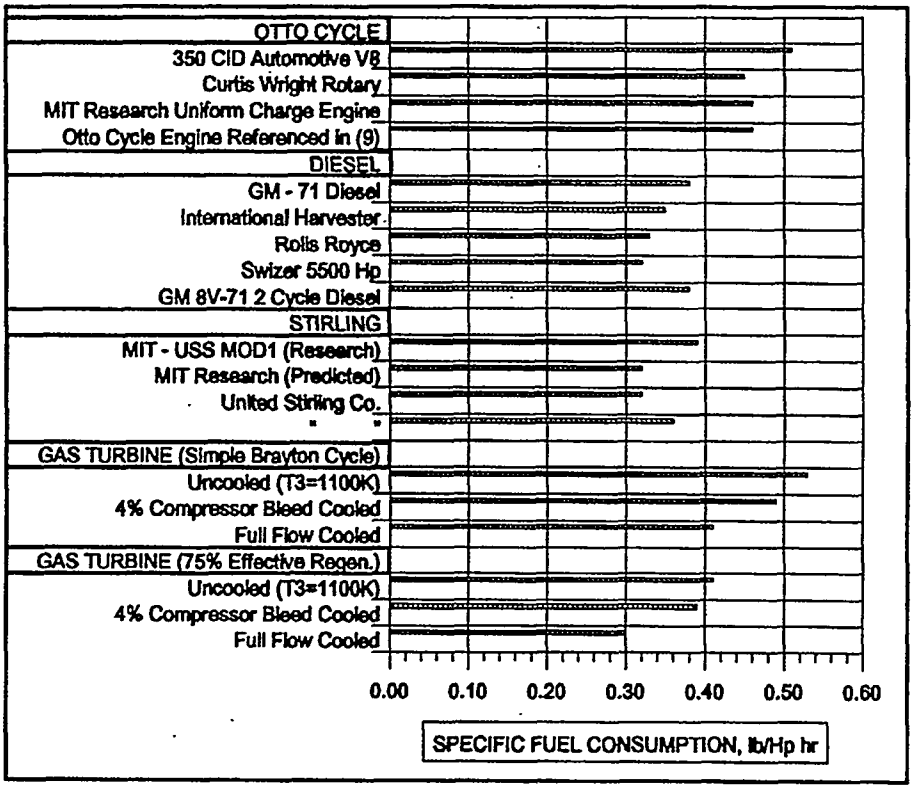

Figure 5. Comparison of specific fuel consumption among various engine types.

* superscripted numbers in parentheses indicate references in Section 7

Figure 5 is a compilation of fuel consumption data for a wide variety of engines. It appears that, in practice, Stirling engines have proven no better than Diesel engines. The highest fuel consumption on the chart is that of an uncooled, unregenerated gas turbine. The full flow cooled gas turbine without regeneration has lower fuel consumption than the gasoline (Otto Cycle) engines, and with 75% regeneration it has the lowest fuel consumption on the chart.

1.5 THE FLOW INTEGRATING SECTION - ERIP INVENTION[11]

1.5.1 Apparent faults in the original full-flow cooling invention.

In a centrifugal compressor with radial vanes about half of the pressure rise takes place in the rotor and half in the diffuser. If the diffuser functions as intended, most of the kinetic energy imparted by the rotor is converted to pressure; however, the diffuser in the original invention seems certain to work very poorly. Figure 6 shows the problem area: The separate streams which flow radially and tangentially from the centrifugal compressor blades into the diffuser would behave as individual free jets rather than a continuous stream. The expansion of free jets into a sudden enlargement is known to be a constant pressure process as the kinetic energy dissipates in turbulence, i.e.. all of the potential pressure rise is lost.

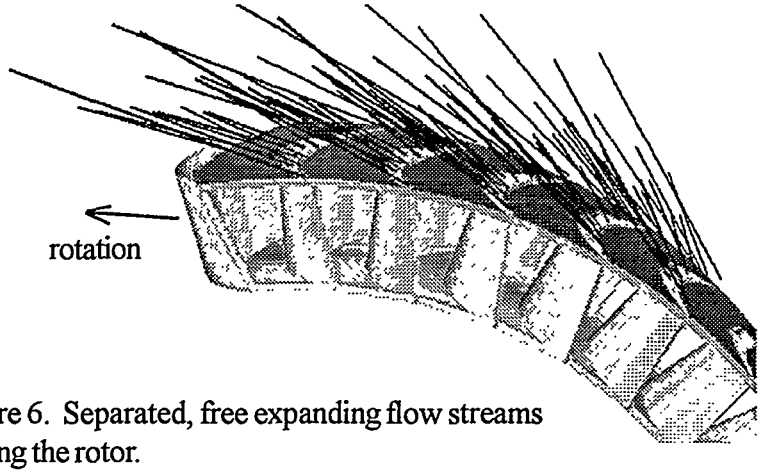

Figure 6. Separated, free expanding flow streams leaving the rotor.

1.5.2 Improvement: A "Flow Integrating Section".

A specially contoured passage placed at the rotor discharge controls the energy dissipating free expansion to the point where the individual streams merge, so that the flow enters the diffuser as a continuous stream. Figure 6 illustrates the concept of the Flow Integrating Section.

* superscripted numbers in parentheses indicate references in Section 7

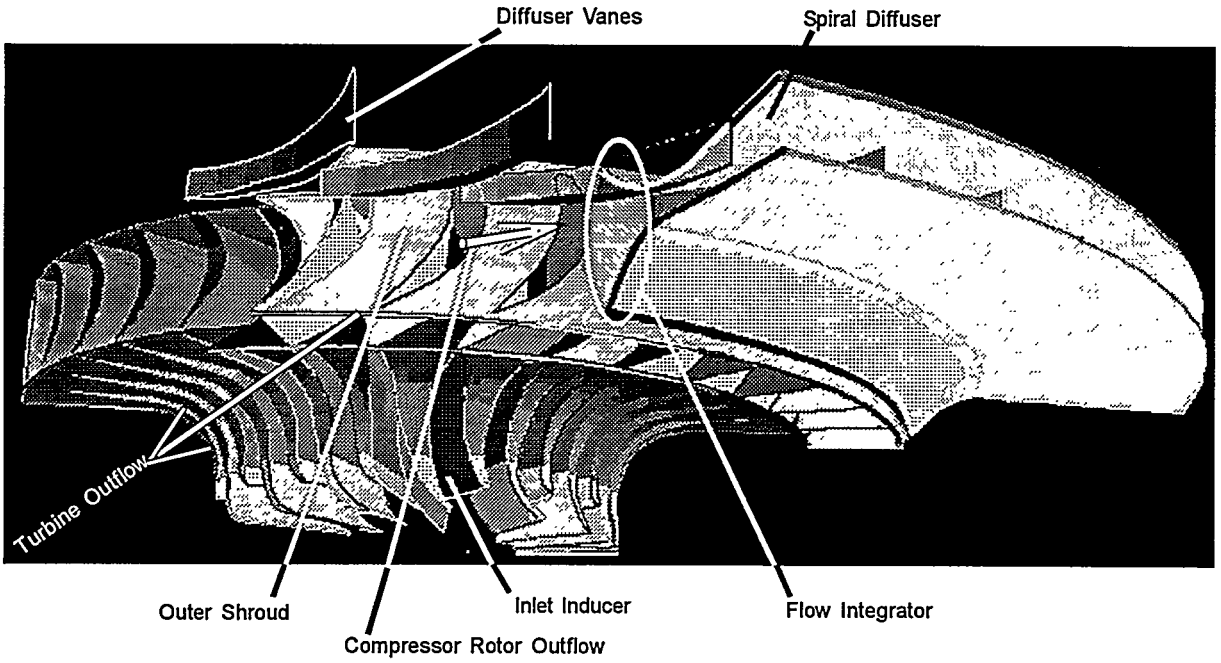

Figure 6. Flow Integrating Section as part of a full-flow-cooled engine.

1.5.3 First Approximation of the Flow Integrating Section Profile.

The first profile approximation was based on a classic boundary layer solution for the velocity profile in a two dimensional free turbulent jet by Goertler[11]. Briefly, the shape of the FIS (Flow Integrating Section) is such that the axial contraction of the FIS passage compensates for the circumferential expansion of Goertler's free jet, i.e. the jet flow cross section supposedly remains constant with radius. The axial width of the FIS passage inlet is equal to the inlet jet width and the axial width at the FIS discharge is equal to the sum of all the inlet jet areas divided by the circumference at the FIS discharge. Figure 7 is an example of the resulting FIS profile.

(r-r0)-cm	Z-cm
0.0	1.42
0.051	1.08
0.102	0.873
0.152	0.733
0.203	0.632
0.254	0.555
0.305	0.495
0.356	0.447
0.406	0.408
0.457	0.375
0.508	0.347
0.559	0.323
0.610	0.302
0.660	0.284
0.711	0.268
0.762	0.253

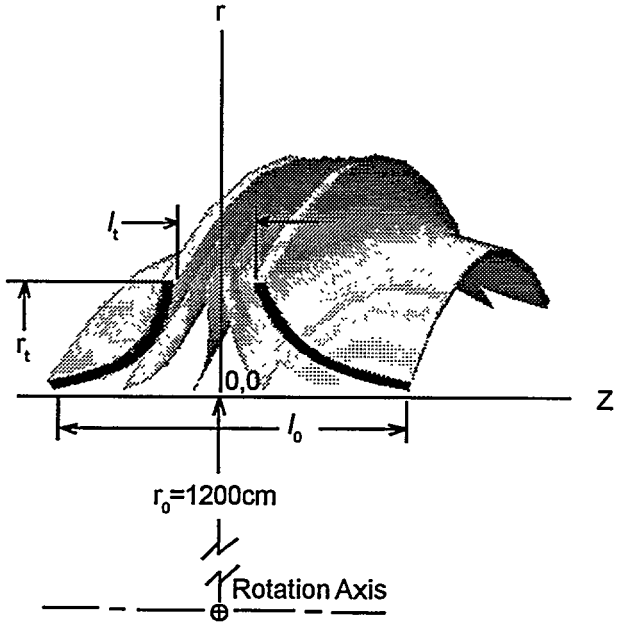

Figure 7. Flow Integrator cross section for the example engine.

* superscripted numbers in parentheses indicate references in Section 7

2. THE ERIP PROJECT

The objective of the ERIP project[12] is to develop optimum design criteria for the Flow Integrating Section. The work is now complete as far as obtaining the necessary data and developing FIS design criteria. The two main aspects of the ERIP project were: (1) computational modeling of three dimensional, turbulent, compressible flow in a series of FIS geometries, and (2) construction, instrumentation, and experimental testing of an apparatus simulating the flow in four different FIS geometries and one configuration without a FIS. The software purchased for this analysis is a computational fluid dynamics package, CFD2000 with the Stormview Post Processor[4] by Adaptive Research. It is a three dimensional, turbulent Navier Stokes solver, which can use a variety of turbulence models (the "KE" model was used in this work). The experimental apparatus was constructed in the FTE prototyping shop, and tested at Colorado Engineering Experiment Station (CEESI)[5] in Nunn Colorado.

2.1 ERIP PROJECT – CFD (Computational Fluid Dynamics Modeling)

2.1.1 Single Channel, Radial Flow. The first attempts at CFD were models of single flow channels. The advantage of modeling a single channel is that it greatly reduces the computation and permits one to use a highly refined computational grid and still reach solution convergence in a reasonable length of time. These simplified solutions showed the flow into suddenly enlarged areas with great detail including the formation of eddies, but the solutions were only valid for pure radial flow. In spiral flow one does not know exactly where the symmetry boundaries between channels are located, while in radial flow the symmetry boundaries are radial planes. One of the first FIS profiles modeled is shown in Figure 8. Note: only the outer FIS wall is curved - like the experimental apparatus.

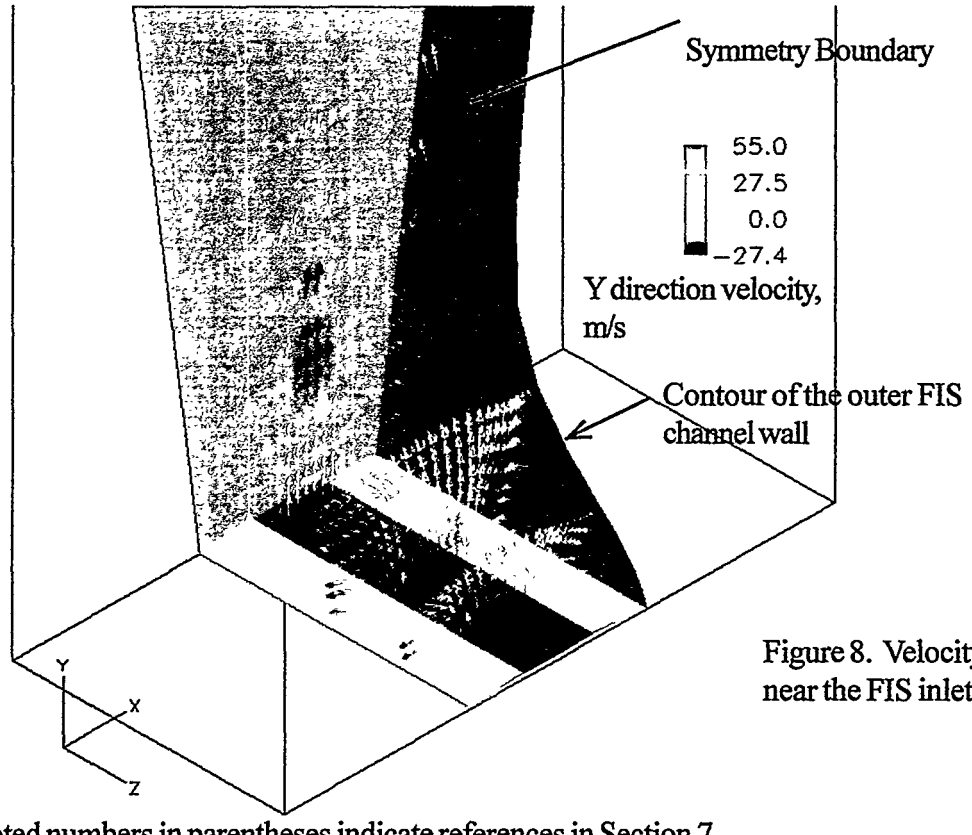

Figure 8. Velocity vectors near the FIS inlet - run X7

* superscripted numbers in parentheses indicate references in Section 7

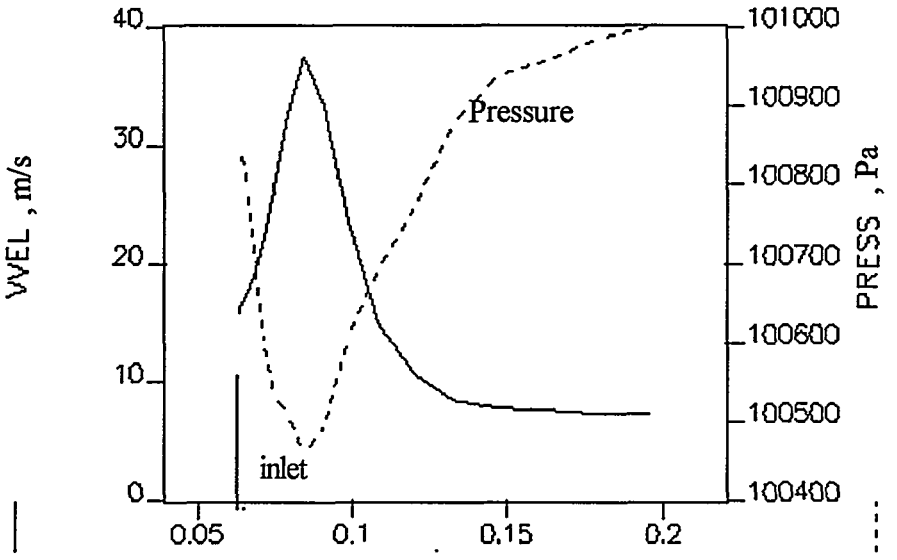

Figure 9. Velocity and pressure distribution with radial distance -- Single Channel Radial Flow. Run X7.

Figure 8 illustrates the eddies which form due to the sudden area enlargement at the FIS inlet. Figure 9 shows that the velocity increases, then decreases in the radial direction; correspondingly the pressure drops, then rises. This behavior is like flow through a converging-diverging nozzle and indicates that the FIS converges too quickly - convergence in the axial direction is greater than the free expansion in the circumferential direction. The diffusion efficiency of this FIS profile is about the same as with no FIS present, around 29%. It is clear from these data that the entrance of the FIS should be tangent to the approaching flow, not like the first approximation, Figure 7. The discharge of the FIS in Figure 7 is, as it should be, parallel to the flow axis, since it is the transition from a converging FIS to a diverging diffuser.

FIS Shape Description: In order to investigate the effect of the FIS shape on performance it is necessary to be able to describe the shape with an expression having a small number of parameters, and satisfy the foregoing requirements. The following expression satisfies all of the requirements:

$$Z(Y) := (1 - C_3) \cdot e^{-C_1 \cdot Y^2} + C_2 \cdot Y^2 + C_3$$

Z is the passage height, and Y is the radial distance from the FIS entrance. The lengths Z and Y are non-dimensional, the normalizing factor being the height at the FIS entrance.

The parameter C1 adjusts the steepness of the wall curve. Another parameter, Arat (area ratio), is the ratio of the inlet jet flow area to the area where the FIS merges with the diffuser. Arat is used to determine the passage half-height, z, at the merge point where dz/dy=0. The specified values of C1, Arat, and the entrance passage height completely determine C2, C3 and the FIS shape. The values of C1 and Arat for the first approximation, Figure 7 would be roughly 40 and 1.0 respectively. CFD computations and experimental tests indicate that this value of C1 may be near optimum when the ratio of distance between jets to jet width (Rgap) is very large. However, as discussed above, the entrance approach must be made parallel to the flow to avoid impact.

* superscripted numbers in parentheses indicate references in Section 7

The effectiveness of the FIS is judged by the overall diffusion efficiency. Adiabatic diffuser efficiency is defined as: (Note: SI units are used throughout this report).

$$\eta_d := \frac{P_2 - P_1}{\left(\frac{\rho_1 \cdot V_1^2}{2}\right) - \left(\frac{\rho_2 \cdot V_2^2}{2}\right)}$$

P_1 = inlet pressure
P_2 = discharge pressure
ρ_1 = inlet density
ρ_2 = discharge density
V_1 = inlet velocity
V_2 = discharge velocity

Single Channel CFD Results. Figure 10 shows the results of single channel radial flow computations on seventeen models in which CD1 varied from 100 to 10,000, Arat varied from 0.32 to 1.0. (Note: CD1 is a dimensional quantity. The dimensionless C1 = CD1 * $6.45*10^{-4}$)

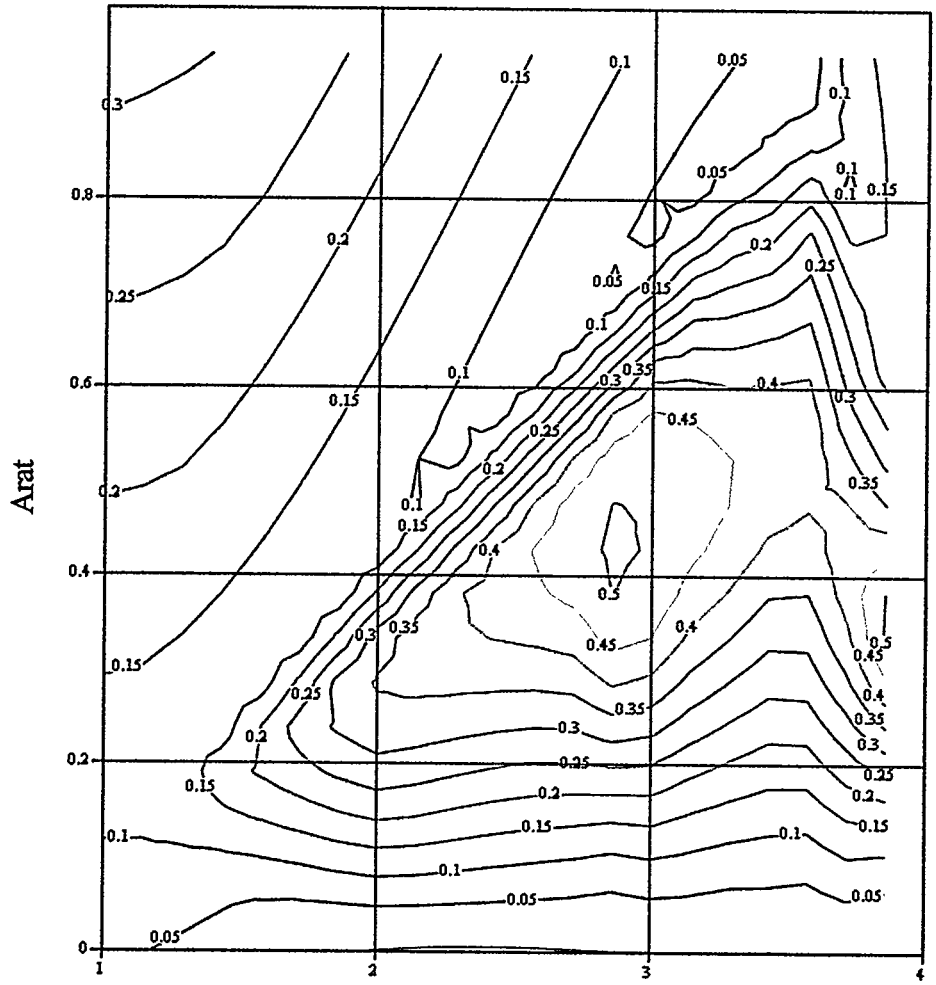

Figure 10. Radial flow efficiency in single channel models. Note: The reversal of slope in the upper left quadrant and the right edge is due to a deficiency of data points in those areas and should be disregarded.

* superscripted numbers in parentheses indicate references in Section 7

2.1.2 Multiple Channel CFD Modeling of Spiral Flow.

It should be noted in Figure 10 that the peak efficiency in the single channel radial flow computations is only 50%. The relatively low efficiency is due to flow separation and eddies formed at the FIS inlet. The actual flow in a centrifugal compressor vaneless diffuser would never be radial because purely radial flow would mean that the rotational speed was zero. In compressor design the radial air velocity and the wheel tangential speed are linked. A rule-of-thumb is that, at design conditions, the ratio of tangential velocity to radial velocity should be around 2.0 to 4.0. Individual particles of fluid tend to obey the law of conservation of angular momentum even if they are not a part of a continuous stream, i.e. the tangential component of velocity varies inversely as the radial distance from the axis of rotation. Therefore, when the radial velocity component of particles of fluid near the FIS entrance slow down (or stop, and reverse direction, as they do when eddies are forming), the total velocity vector turns toward the tangential direction, becomes tangential, and turns inward toward the rotation axis. The net result is that the free jet entering the FIS turns sharply toward the tangential direction. The turning is beneficial in two ways: (1) geometrically it causes the adjacent streams to merge quickly (2) it brings high velocity cooling air closer to the between-blade shrouds which otherwise might be in a poorly cooled stagnant region. Figure 11 clearly shows the bending of the path lines.

Figure 11. Path lines of flow from one of the twenty four inlets. Run X85_MI.

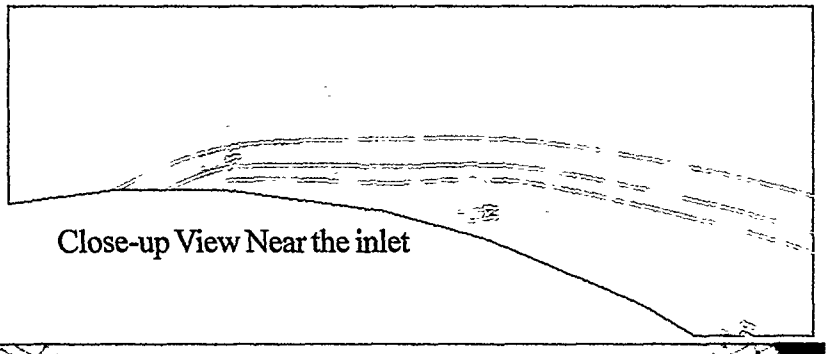

Close-up View Near the inlet

Through the FIS and diffuser.

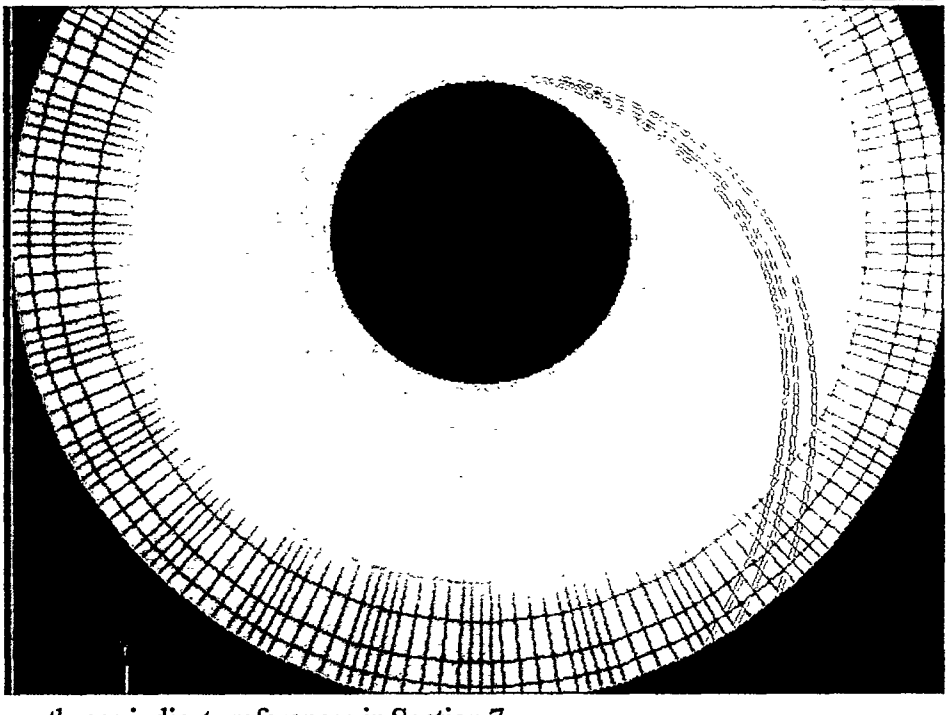

* superscripted numbers in parentheses indicate references in Section 7

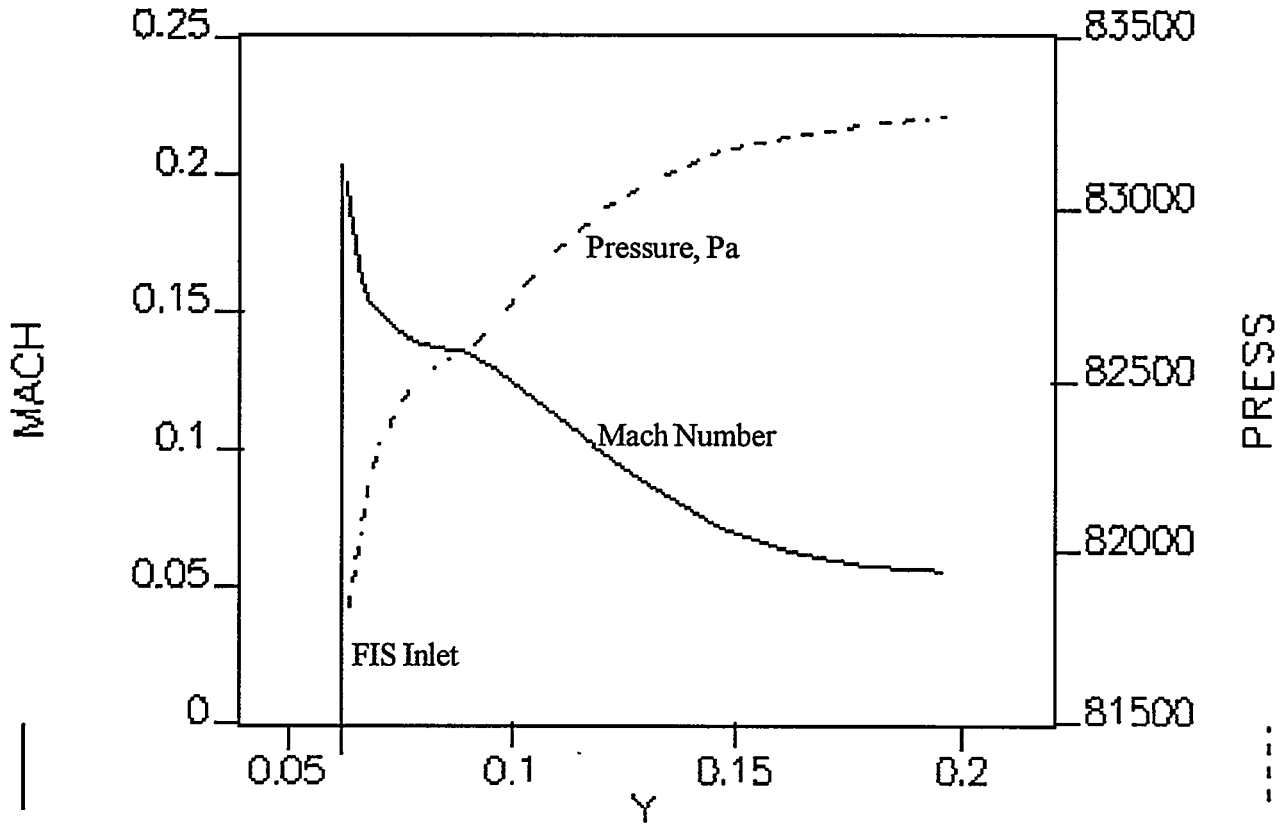

Figure 12 Mach Number and pressure variation with radial distance. Run X85k_MI

Note, in contrast to Figure 9 the Mach Number drops steadily except for a leveling out at the FIS discharge (diffuser entrance). The pressure rises with no sign of flow separation. In this run C1=3.23 and Arat=0.8, the diffusion efficiency was 84%.

2.2 ERIP PROJECT – EXPERIMENTAL PHASE

Since the flow in a stationary FIS and diffuser was the subject of ERIP study there was no need for a rotating impeller. The flow being discharged from a rotor can be simulated by a set of stationary turning vanes. The construction is shown in Figure 13. Since the flow tests were to be done at room temperature and flow visualization by means of smoke injection seemed desirable, most of the apparatus was made of Lucite. The turning vanes were cast in long strips of Polyester Resin using stainless steel tubing as molds. Individual blades were cut and held in position for adhering to the Lucite base by an indexing jig.

* superscripted numbers in parentheses indicate references in Section 7

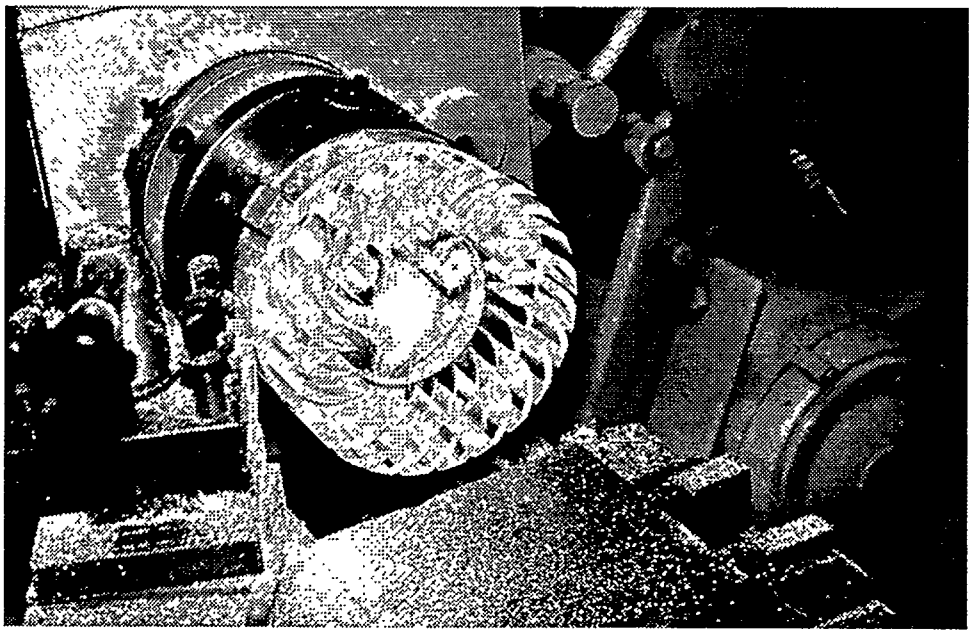

Figure 13. Inlet turning vanes being trimmed and faced.

A variety of FIS passage profiles were formed by shaped inserts which could be easily changed from one test to the next. The inserts were made of high density foam machined in the lathe to the desired surface contour by means of a die grinder attached to a pantograph. The pantograph was designed to use 2X scale templates to improve the accuracy of the surface contour. Finally each shaping insert was coated with hard epoxy and sanded smooth.

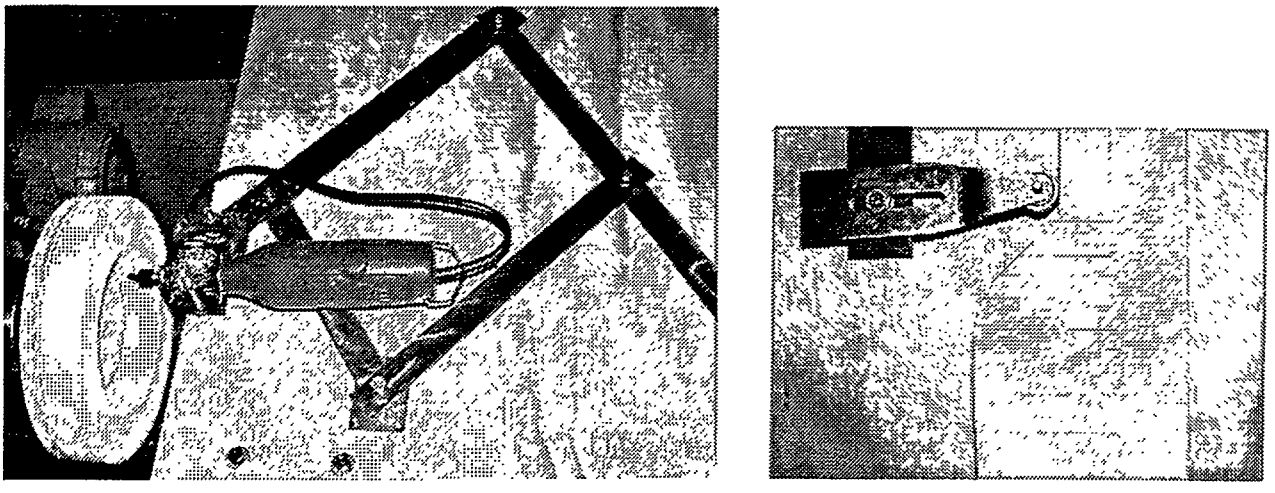

Figure 14. Machining of FIS shaping inserts.

* superscripted numbers in parentheses indicate references in Section 7

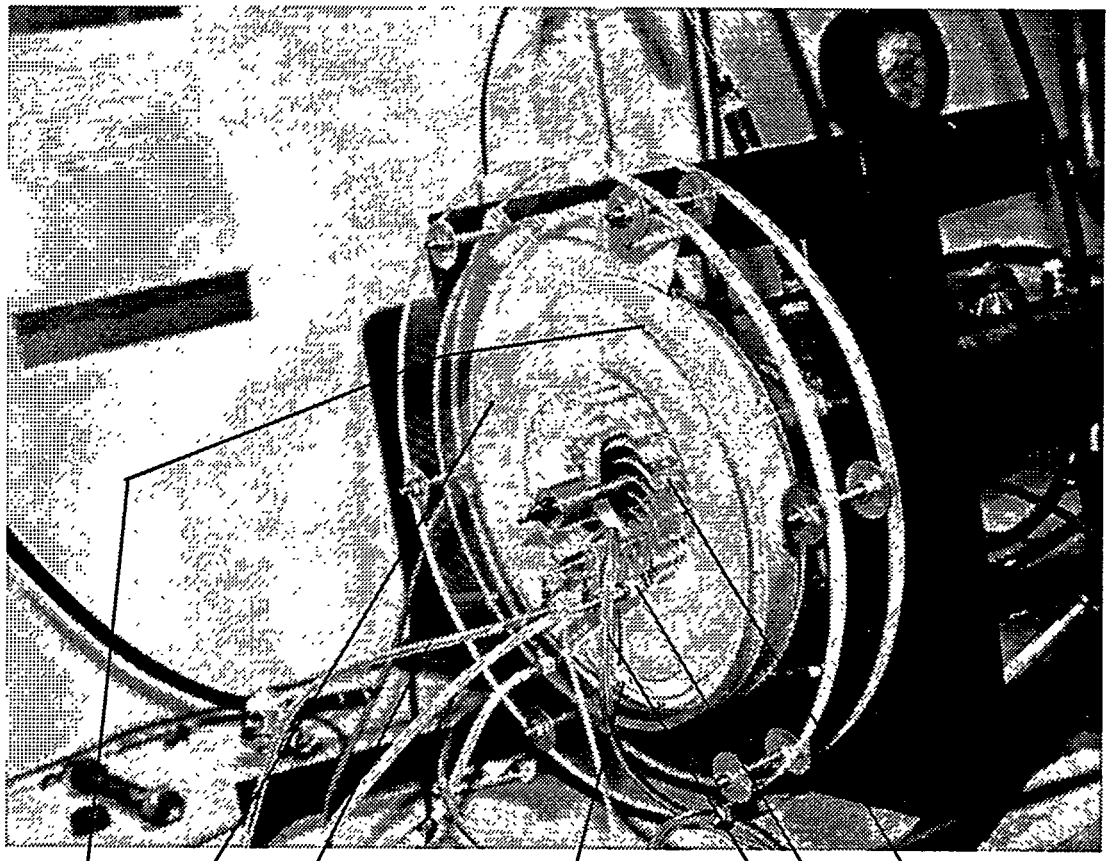

Figure 15. Test apparatus installed at CEESI

* superscripted numbers in parentheses indicate references in Section 7

Experimental Results

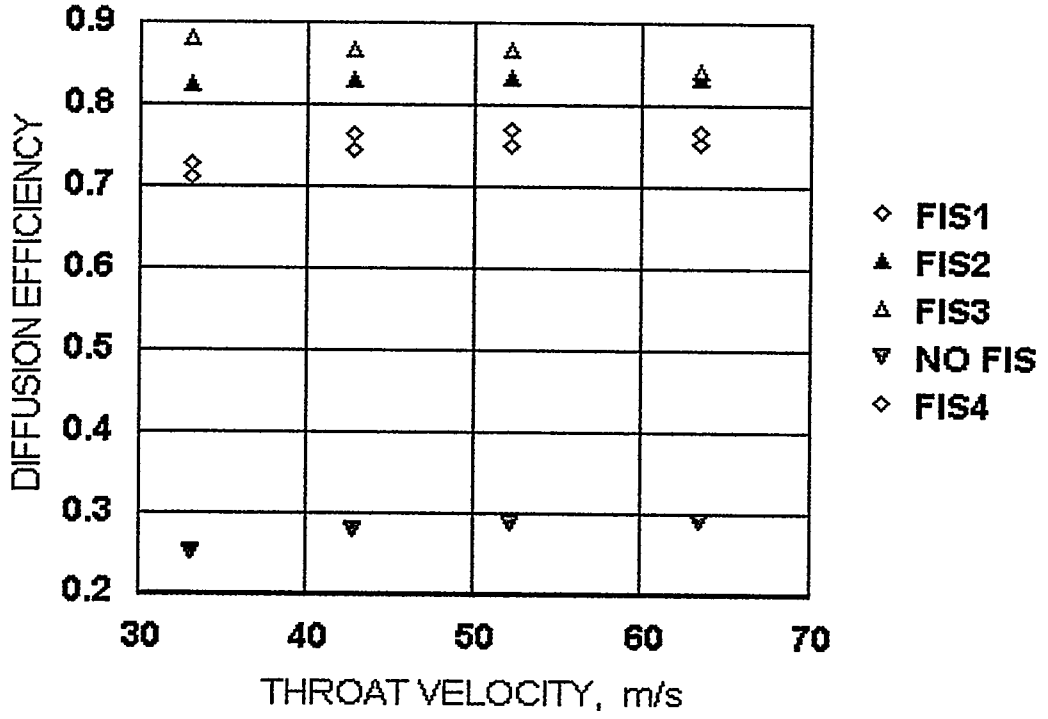

Figure 16. The "FIS" numbers refer to the FIS shape inserts:
FIS1 - C1=3.23, Arat1=1.0 FIS2 - C1=3.23, Arat1=0.6
FIS3 - C1=3.23, Arat1=0.8 FIS4 - C1=3.23, Arat1=0.32
NO FIS - Flow Integrating Section removed.

Experimental vs. Computational Comparisons

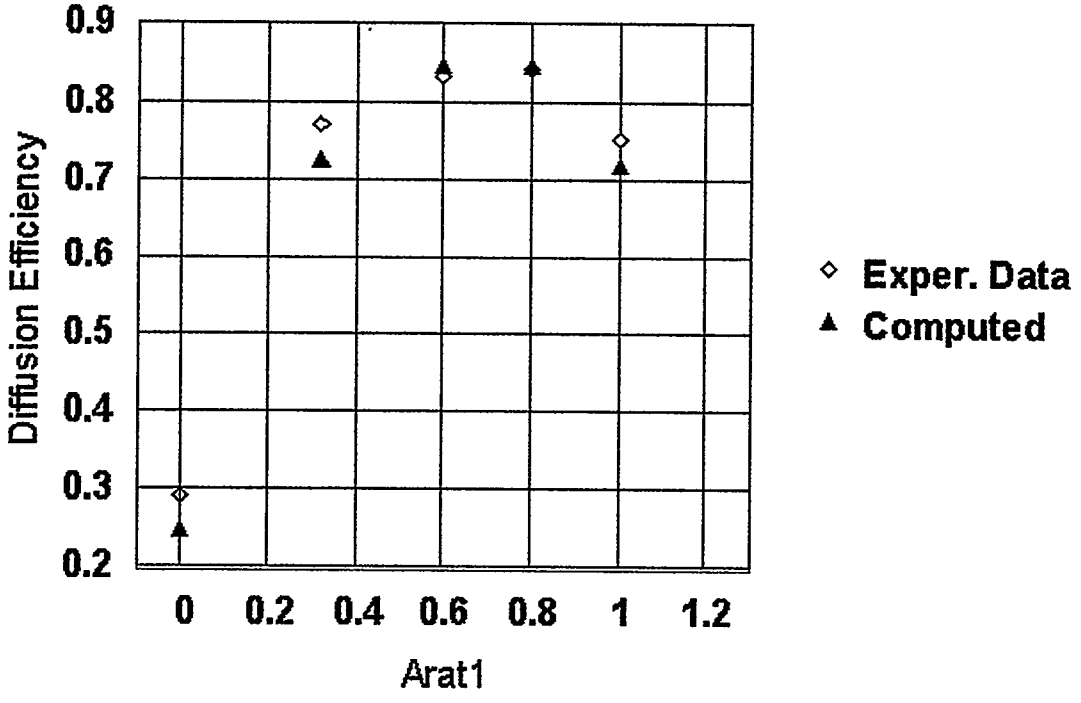

* superscripted numbers in parentheses indicate references in Section 7

2.3 COMPARISONS OF COMPUTED AND EXPERIMENTAL RESULTS

The comparisons made in Figure 14 show that CFD analysis can be used with good accuracy in predicting the performance of variations of the Flow Integrating Section.

3. COMMERCIAL POSSIBILITIES AND SPECIAL CONSIDERATIONS FOR VERY SMALL ENGINES.

The ultimate application visualized for this gas turbine engine is a hybrid, turbo-electric vehicle, the heart of which is a turbine driven generator. The qualities claimed for the subject turbine engine – light weight, high power density, simplicity, and outstanding fuel economy would make it particularly suited for vehicle applications. Except for the non linear effects of size, the engine and FIS design do not depend on the application.

A large market already exists for engine driven generators of all sizes and applications ranging from hand-carried portable power supplies to propulsion for trucks, locomotives, and ships – as well as hybrid automobiles. FTE has responded to a DOD solicitation for a turbo-electric auxiliary power plant of at least 10kw, which must weigh less than 75 pounds. The small sized (around 20 horsepower) engine required for this application poses a real challenge. A simple scaling down from a previous 300 horsepower design of five inch diameter to 20 horsepower would result in a wheel of only 1.3 inch diameter spinning at nearly 200,000 rpm to attain the same pressure ratio. Some modifications which would alleviate the excessive speed would be: a) increase the wheel diameter as much as possible (performance of the FIS and diffuser will limit this size), b) add a second turbine/ compressor stage, c) compromise for a lower pressure ratio, hence, lower efficiency.

The proposed engine configuration is shown in Figure 15 below. The rationale behind the secondary, free wheeling, counter-rotating stage design is outlined following the figure.

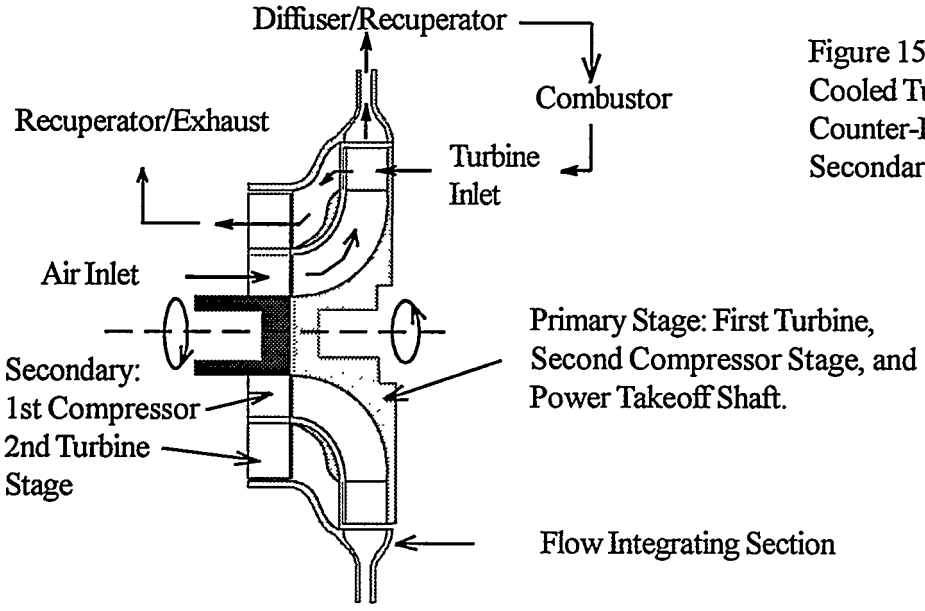

Figure 15. Schematic of Full Flow Cooled Turbine Engine with Counter-Rotating, Free-Wheeling Secondary Stage.

* superscripted numbers in parentheses indicate references in Section 7

Some of the advantages of a counter-rotating, free-wheeling secondary stage relative to a single stage, are:

1) The desired compression ratio can be obtained at a lower rotational speed.

2) The first stage turbine can be more highly loaded, i.e.. the gas turning angle can be greater, and more power delivered to the output shaft. In a single stage axial flow turbine the best efficiency is obtained when the turbine discharge absolute velocity is axial. A second turbine stage rotating in the opposite direction can utilize backspin from the first stage, and the second stage can discharge axially as desired for best overall efficiency.

3) Engine torque-speed characteristic and control stability should improve. A conventional gas turbine engine has poor operating characteristics in that a small increase in load can quickly slow down and stall the engine, or cause wild fluctuations in the fuel control which is trying to maintain the speed while avoiding over-temperature. The increased load slows the turbine and attached compressor so that the output pressure and mass flow drop, hence torque, power, and speed tend to drop off quickly. The fuel controller attempts to correct by increasing fuel flow, but with the reduced mass flow the turbine inlet temperature rises sharply, quickly reaches its limit, and the engine stalls.

When the counter-rotating stage is present, the load increment again tends to slow the power output shaft slightly, but this time the slowing causes the backspin from the first stage turbine to increase in velocity which speeds up the secondary wheel because it rotates in the opposite direction. The secondary wheel is free to speed up because it is not directly connected to the load. The first stage axial compressor which is part of the secondary wheel also speeds up. Not only does the first stage increase its pressure output and mass flow, but the spin of air exiting that compressor stage increases such that it compensates for the reduced speed of the centrifugal compressor, helps maintain the correct angle of attack, and tends to maintain its pressure output. Since the mass flow has increased, the turbine inlet temperature tends to drop. The fuel controller senses both a speed and temperature drop, so it increases the fuel flow and power increases correspondingly to meet the load increment while the temperature returns to its set value or increases only slightly. This type of operation is inherently stable, while that previously described was inherently unstable. Of course, as with any engine, there are limits to the viable range of operation. In the second case described, a limitation is likely to be due to the possibility of overspeeding the secondary wheel. Secondary wheel speed will have to be monitored and limited to safe values.

4. EFFECTS OF SMALL SIZE ON FIS DESIGN.

SCALING: When an engine of one size (power output) has been designed, one can estimate some of the design parameters for an engine of a different size through a type of scaling which depends on the assumption that compressor pressure ratio, turbine inlet temperature, and efficiencies do not change from one design to the other. The first conclusion is that the mass flow of air through the engine would vary in direct proportion to power. If similar geometry were also assumed, then dimensions such as the wheel diameter would scale as the square root of power and rotation speed would vary inversely as the square root of power. Centrifugal stress would remain unchanged. Thus a 300 horsepower two stage engine with a 5 inch diameter wheel turning 50,000 rpm would scale to a 20 horsepower engine with a 1.29 inch wheel turning at 194,000 rpm!

* superscripted numbers in parentheses indicate references in Section 7

Extremely high rotational speed creates problems for bearings and gear reduction. (Gas bearings might be a possibility.) A direct-coupled generator running at such high engine speed seems unlikely. The small size gives rise to low Reynolds Number (ratio of momentum-to-viscous forces). In the example above, the Reynolds number for the smaller sized engine would be about one fourth that of the larger sized engine, thus gas flow friction losses would be about four times greater. Smaller size also places high demands on precision of manufacturing to prevent excessive leakage losses.

All of the above indicate that, in scaling to a very small engine size:

1) The idealized scaling from a larger size is not always appropriate – pressure ratio, hence efficiency are bound to be lower. Thus, for a given required power, mass flow must be higher. Because gas density is lower and mass flow is higher the engine dimensions increase. Thus, for a given engine power, the physical dimensions of the engine tend not to shrink so drastically as the idealized scaling would indicate when the inevitable efficiency or pressure ratio decrease is considered..

2) The tip diameter of the centrifugal impeller should be made as large as possible, probably exceeding normal design convention. In that way torque is maximized and rotational speed is minimized without changing the power.

EFFECT OF STRETCHING THE COMPRESSOR TIP DIAMETER. A two stage engine such as Figure 15 was scaled from 305 HP to a nominal 50 HP. The mass flow was scaled from 0.824 Kg/s to 0.136 Kg/s. The compressor tip diameter remained 0.127 m (5"), which is approximately 2.5 times the diameter which would have resulted from scaling method described above. This stretching of the diameter is extreme; however, the objective is to test the effect on the performance of the FIS and diffuser. Fifty horsepower was chosen rather than twenty in a first iteration in anticipation of a reduced FIS efficiency which, in the final computation, will reduce the horsepower at the same mass flowrate.

The main effect of diameter stretching on the design and performance of the FIS is to increase Rgap, which is the ratio of gap between blades – to – the width of jet flowing radially outward from each blade. The design procedure which leads to the increase in Rgap is:

1) The tangential tip speed of the centrifugal compressor is determined by the design pressure ratio for that stage. Tip speed corresponding to 50,000 rpm is 333 m/s, temperature of 450 K (after compression), tangential Mach number = 0.79, and a centrifugal stage pressure ratio (assuming 0.84 compressor efficiency) = 2.67.

2) A value of 3.0 was assumed for the ratio of tangential-to-radial velocities, as being toward the high end of conventional practice. Then the radial velocity is 333/3 = 111 m/s. Density is known from the pressure and temperature and from the radial velocity and density the radial flow area turns out to be $1.64(10)^{-4}$ sq m.

* superscripted numbers in parentheses indicate references in Section 7

3) Turbine design considerations involving the stage enthalpy drop, give the gas turning angle, and design charts yield a recommended blade solidity, which is the ratio of blade chord-to-spacing between blades.. Remembering that the inside of a hollow turbine blade is the compressor discharge flow area of a compressor blade, the solidity, wall thickness, density, and number of blades yield a value for Rgap. In the case studied the solidity was 1.43 and the resulting Rgap was 12.3.compared to 2.73 for the 300 HP engine.

Figure 16 Showing the change in the shape of the FIS in going from the 300 HP engine (on the right) to the 50 HP engine (on the left).

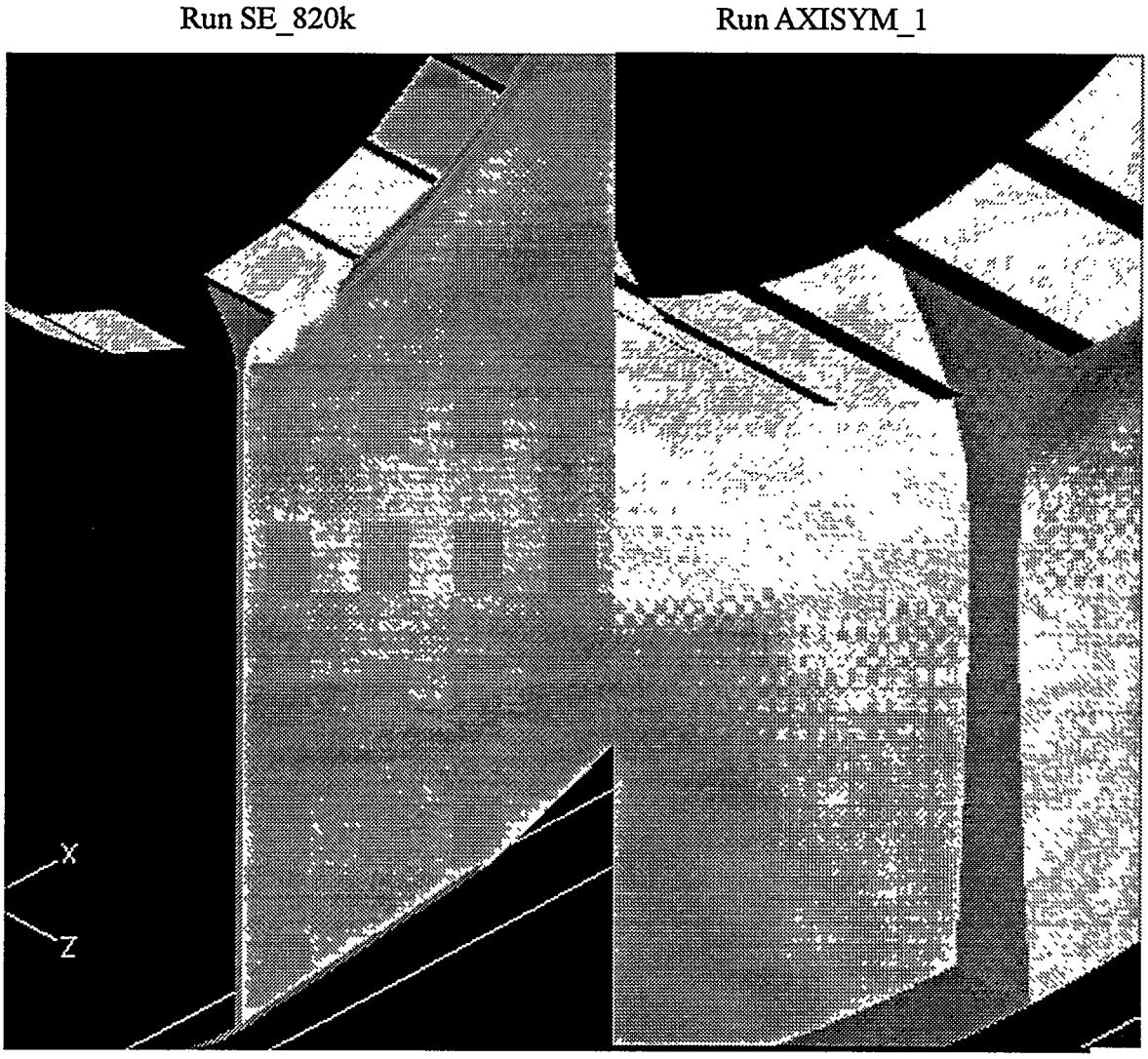

Figure 16 shows the effect on the shape of the FIS caused by attempting to use a much larger diameter compressor impeller than would result from an idealized scaling. The blue slots around the inner circle represent the flow inlets to the FIS. The best diffusion efficiency obtained through CFD modeling was 68%.

* superscripted numbers in parentheses indicate references in Section 7

On the second iteration, when the centrifugal stage diffusion efficiency was reduced from 84% to 68%, the engine efficiency dropped from 39.2% to 31.6% and the horsepower dropped from 50 to 38. Engine efficiency did not drop as much as might be expected, partly because the engine has two compressor stages. The first, axial flow stage, is not affected by the "diameter stretching" which is applied to the second, centrifugal compressor stage, since the first stage is smaller (see Figure 15) and can run at an rpm which is limited only by centrifugal stress. Also, the second turbine stage need not be cooled and would not suffer the heat transfer penalty since the temperature will have dropped sufficiently through the first turbine stage that normal blade materials can operate without cooling.

It appears that an engine of under fifty horsepower could actually be designed with a five inch diameter power takeoff stage operating at 50,000 rpm - a very manageable speed; however, one would anticipate that, after a more thorough design effort, the eventual diameter would be closer to three inches. The efficiency appears quite acceptable; however, much more study would be necessary before a definite conclusion could be drawn. For example, the effects of seal leakage would have to be investigated. In the interest of keeping the size and weight low, the regenerator effectiveness might have to be compromised to some extent, and a turbine inlet temperature of 1,800 Kelvins might be overly ambitious in the early stages of development, particularly in an application where fuel economy is of lesser concern than portability, reliability, and low cost.

5. CONCLUSIONS CONCERNING THE FLOW INTEGRATING SECTION.

The unique configuration of the engine being studied creates a new problem in the area of the compressor diffuser: the flow entering the diffuser is not continuous, but is in the form of an array of individual jets separated by the space between the blades. The flow in free jets is not energy conservative, but dissipates its energy in turbulence. The purpose of the ERIP invention, the Flow Integrating Section (FIS) is to efficiently merge the individual jets into a continuous stream before it flows into the diffuser. The original premise, that diffusion efficiency without a Flow Integrating Section would be unacceptably low, was correct. Figure 16 (upper) shows that the maximum efficiency without a FIS was only 29%.

An initial FIS shape described in S1.5.3 was based on a classical boundary layer solution for free jet expansion. Computational fluid dynamics (CFD) modeling of the flow in a FIS indicated that the initial shape converged much too abruptly and lacks an approach region in which the channel walls are parallel to the entering flow. The shape based on the boundary layer solution assumed that it would be desirable to squeeze the jet in the direction normal to the machine axis to exactly compensate for its free expansion in the tangential direction, thus theoretically allowing no diffusion in the FIS. The CFD results showed that the FIS flow is not just a boundary layer problem, and when wall constraints are placed on two sides of the "free jet" it no longer behaves as a free jet. The dynamics, such as angular momentum of the core flow change the flow structure, and a turning into the swirl direction causes adjacent jets to interact almost immediately, so free jet flow is not very relevant.

* superscripted numbers in parentheses indicate references in Section 7

An equation to describe the shape of the FIS is discussed on page 11. The equation contains a parameter, C1 which affects the steepness of wall convergence, and Arat1 which is the ratio of the inlet jet flow area to the area where the FIS merges with the diffuser. Specification of C1, Arat1, and the entrance passage height completely determine C2, C3, and the FIS shape. The present data indicate that FIS shape parameters C1=3.22 and Arat=0.75 are approximately the optimum values. Whether these values are universal remains to be seen, but they should at least be good starting values for CFD analysis of new designs. The best efficiency at 64 m/s throat velocity is 84%. For comparison, in Figure 17 are compressor diffuser design curves from reference [6].

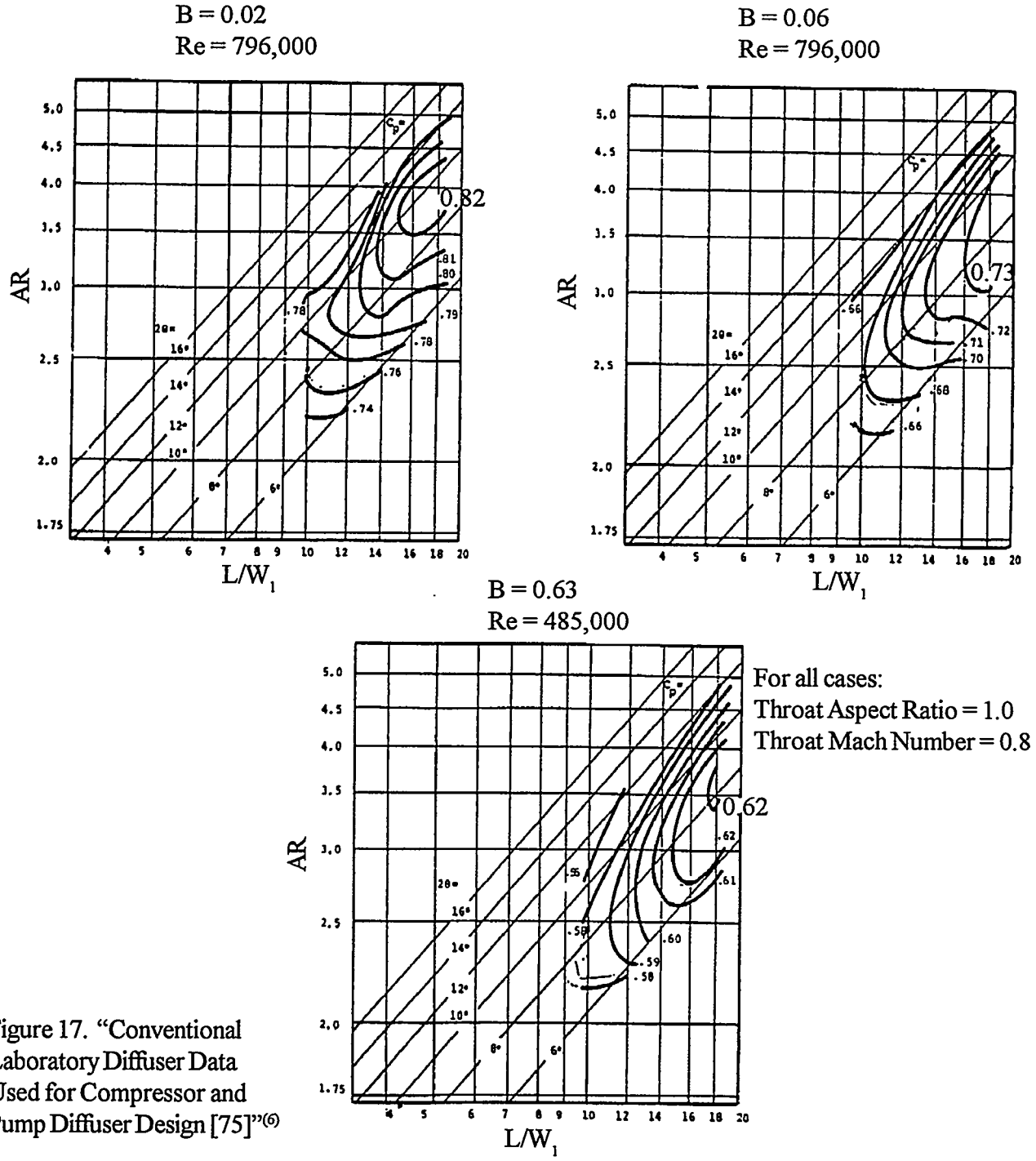

Figure 17. "Conventional Laboratory Diffuser Data Used for Compressor and Pump Diffuser Design [75]"[6]

* superscripted numbers in parentheses indicate references in Section 7

For comparison of the CFD and experimental models with the data of Figure 17:

AS, aspect ratio = 0.75 (varies)
AR, area ratio = 3.13 (all models)
B, aerodynamic blockage. B is a measure of boundary layer thickness at the diffuser entrance. One can only say that it should be very small because the Reynolds number is large, the flow is accelerating locally, and the distance for boundary layer growth is very small. Estimated B < 0.02.
Re, Reynolds' number = Density X Velocity X Throat depth / Viscosity = $2.8(10)^5$ to $7(10)^5$ based on hydraulic diameter.
L/W_1, diffuser length-to-width (flow path length / throat height) = 17 (average)
2Θ, = divergence angle = 7 deg (equivalent cone angle)

As can be seen in Figure 17, the best efficiency contour shown is 82% efficiency for conventional diffuser configurations; whereas, the FIS - diffuser combination of this study achieved 84%, both computed and experimental. Without a FIS the efficiency dropped to 29%. Therefore, it would seem safe to conclude that a properly designed Flow Integrating Section prevents the diffuser pressure losses which would arise from the full turbine blade cooling configuration, if the FIS were not present.

A special case was investigated: a very small engine designed with a much larger than "normal" centrifugal impeller diameter in order to reduce the design rotational speed. Additional measures to reduce speed were the addition of a second turbine/compressor stage, and a reduction of design pressure ratio. The main effect on the flow geometry was that the ratio of blade spacing – to – the width of the blade jet stream, Rgap, increased from 2.73 for the "normal" design to 12 when the diameter was stretched from 1.29 inches to 5.0 inches. The quadrupling of Rgap had a deleterious, but not disastrous effect on the diffusion efficiency. The diffusion efficiency dropped from 84% to 68%. Correspondingly the computed engine efficiency dropped from 39.2% to 31.6% assuming all the same regenerator effectiveness, and turbine efficiency. The rotational speed dropped from 194,000rpm for the 1.29 inch wheel to 50,000rpm for the 5 inch wheel. While this stretching of the wheel diameter is probably too drastic, the results show that a small engine might be designed with reasonable rotational speed, and the FIS will continue to be effective. The new data indicate that the optimum value of C1 would increase from 3.2 for Rgap = 2.73 to around 3.9 for Rgap = 12, and the optimum value of Arat1 does not change appreciably.

6. COMMERCIALIZATION

The commercial possibilities for small turbo-generators are discussed in Section 3. The DOD SBIR support for constructing a prototype turbo-electric auxiliary power unit would be an excellent opportunity to demonstrate a full-flow-cooled turbine engine with the Flow Integrating Section. An important goal of the Phase I will be to contact engine manufacturers who might be interested in participating in Phase II – the actual construction of a prototype. If the results were good there would seem to be a real possibility that an industrial participant in an SBIR Phase II project would be interested in becoming a commercialization partner – one with the necessary manufacturing capability.

* superscripted numbers in parentheses indicate references in Section 7

7. REFERENCES

1. W. Gene Steward, COMPACT GAS TURBINE ENGINE WITH EFFECTIVE TURBINE BLADE COOLING; FINAL REPORT, SBIR Phase I Contract NAS3-26139, (July 17, 1991), To: NASA Lewis Research Center, 21000 Brookpark Road, Cleveland, OH 44135, Attn. R.J. Roelke.

2. S. Helou, (French patent - two pages, not including title or date, supplied by the US patent office in response to this author's patent application.) (circa 1950)

3. T. R. Schulz, POWER PLANT COMPRISING A TOROIDAL COMBUSTION CHAMBER AND AN AXIAL FLOW GAS TURBINE WITH BLADE COOLING PASSAGES THEREIN FORMING A CENTRIFUGAL AIR COMPRESSOR, US patent #2m611m241m (Sept. 1952)

4. Adaptive Research Co., Santa Monica, CA, CFD2000 COMPUTATIONAL FLUID DYNAMICS SOFTWARE / STORMVIEW POST-PROCESSOR. Perpetual lease (Aug. 1997)

5. Colorado Engineering Experiment Station, Nunn, Colorado.

6. J.W. Sawyer, and D. Japikse (editors), SAWYER'S GAS TURBINE ENGINEERING HANDBOOK, (3 volumes) Turbomachinery International Publications, Division of Business Journals, Inc., 22 South Smith Street, Norwalk, CT 06855, (1985)

7. W. H. McAdams, HEAT TRANSMISSION, McGraw-Hill, New York, (1954)

8. W.W. Bathie, FUNDAMENTALS OF GAS TURBINES, John Wiley & Sons, (1984)

9. T. Baumeister, E.A. Avallone, and T Baumeister III, MARKS' STANDARD HANDBOOK FOR MECHANICAL ENGINEERS, 8th edition, McGraw-Hill, New York, (1978)

10. W.R. Martini, WHENCE STIRLING ENGINES, 17th ICEC, CH1789-7/82/0000-1669, (1982)

11. H. Schlichting, BOUNDARY LAYER THEORY, fourth edition, McGraw-Hill, (1962)

12. W. Gene Steward, FLOW INTEGRATING SECTION FOR A GAS TURBINE ENGINE IN WHICH TURBINE BLADES ARE COOLED BY FULL COMPRESSOR FLOW, DOE - ERIP (Energy Related Invention Program), Contract #DE-FG01-97EE15668 (Aug. 1997). Project Officer: David Crouch, U.S. DOE, 1000 Independence Ave. SW, Washington, DC (202)586-4844

* superscripted numbers in parentheses indicate references in Section 7